Electronic Supplementary Material (ESI) for Energy & Environmental Science.

Supplementary Information

Exogenous Electricity Flowing through Cyanobacterial Photosystem I Drives CO_2 Valorization with High Energy Efficiency

Zhaodong Li, Chao Wu†, Xiang Gao†, Bennett Addison, Shrameeta Shinde, Xin Wang, Xihan Chen, Jianping Yu, Drazenka Svedruzic, Jeffrey Blackburn*, Wei Xiong*

Correspondence to: Wei.Xiong@nrel.gov (W.X.), Jeffrey.Blackburn@nrel.gov (J.B.)

This PDF file includes:

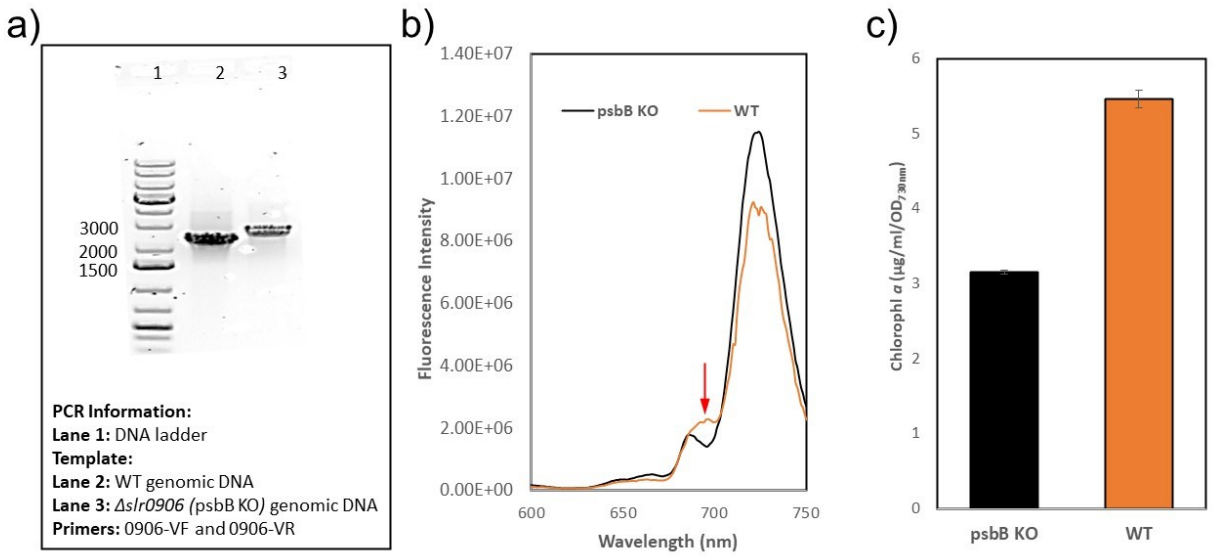

Fig. S1. Genotype and phenotype of PSII knockout mutant. a) PCR analysis verified that psbB gene was interrupted by a larger size streptomycin gene cassette replacing partial coding region; b) 77K fluorescence demonstrated disappearance of a shoulder peak at 695 nm (indicated by a red arrow) due to the psbB deficiency; c) Chlorophyll *a* concentrations in the mutant and wild type. Error bars represent biological triplicates.

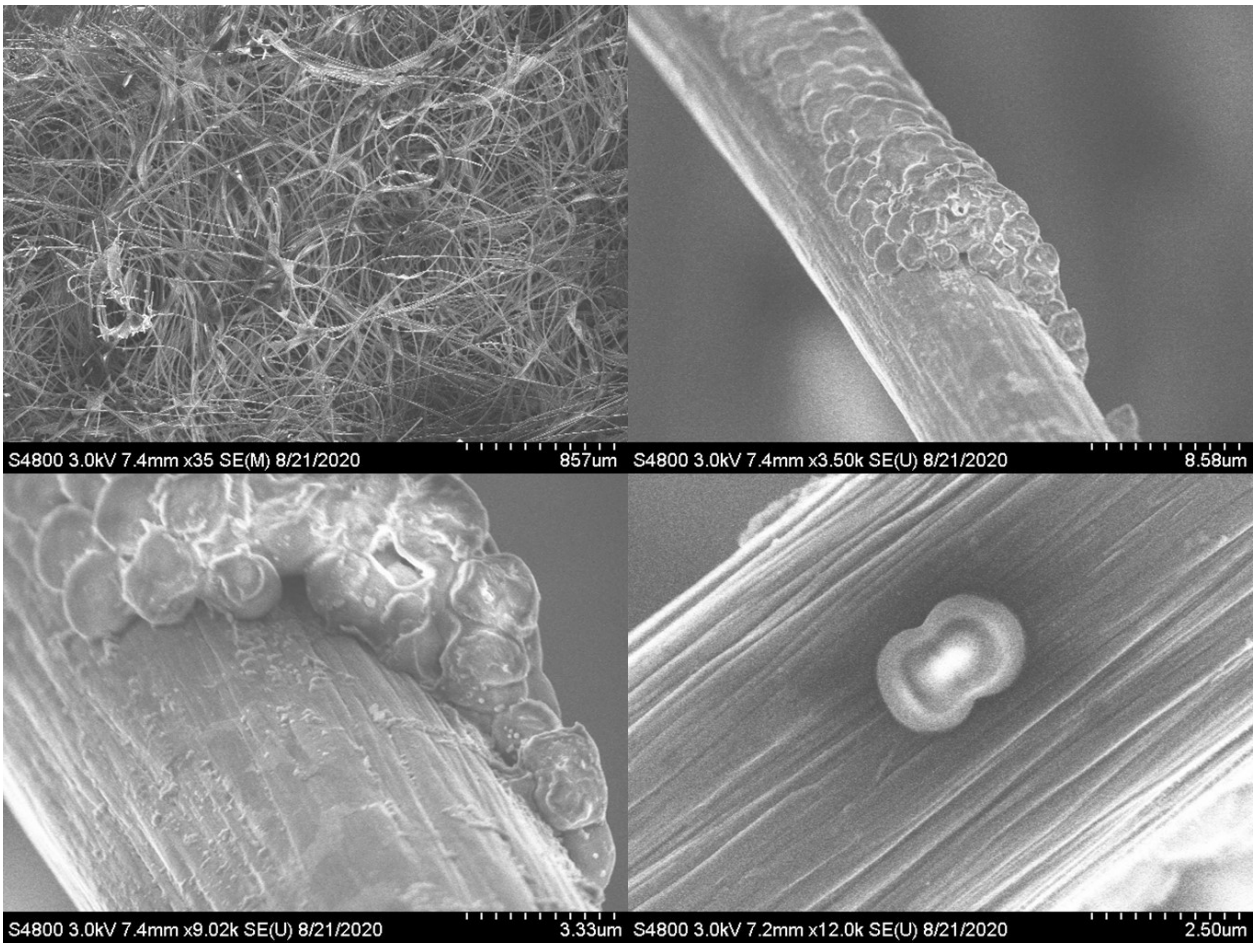

Fig. S2. Scanning electron microscopy (SEM) of PSII-deficient *Synechocystis* cells on carbon felt electrode materials in different magnifications.

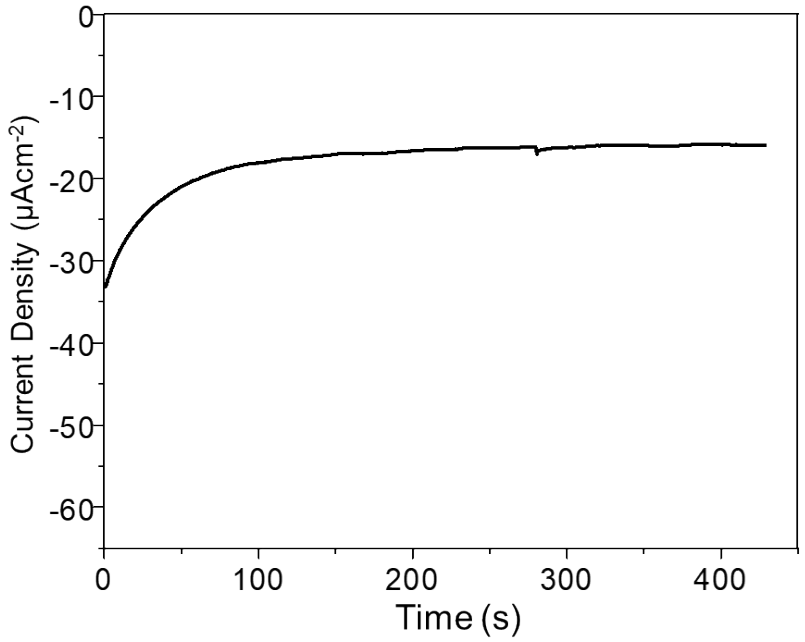

Fig. S3. The current response of culture with the dead PSII mutant cells under the same chopped illumination condition as the result shown in Fig. 2a. In order to ensure a reliable comparison, the electrolyte components are same as those used for the culture in Fig. 2a. The cells were killed by heating the culture at 50 ^{o}C for 16 hours. The electrochemistry experiments were conducted for 5 times and the representative result was shown here.

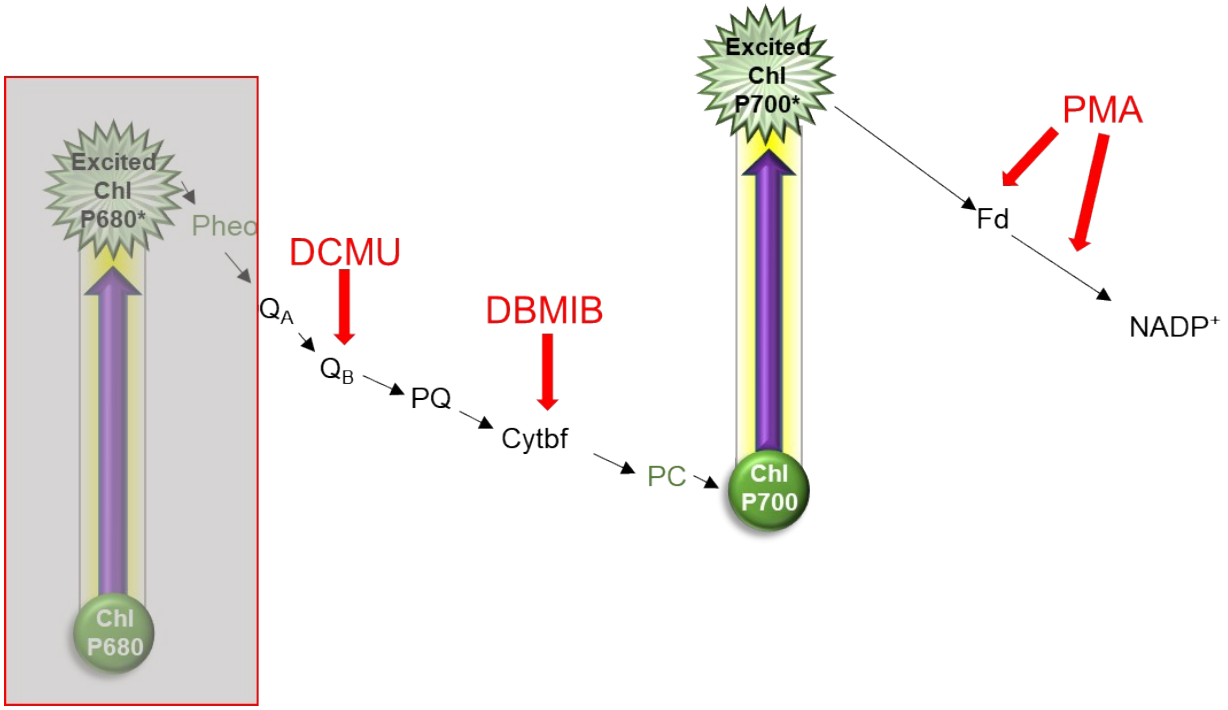

Fig. S4. Site-specific inhibitors act on the "Z" scheme of natural photosynthesis. Gray bar indicates the deficient PSII. Three inhibitors: DCMU, DBMIB, and PMA inactivate the Q_B, Cytochrome b6f complex, and components downstream of PSI in the PETC, respectively.

Fig. S5. Pathway enzyme allocation in the proteome of electrophototrophic *Synechocystis* ΔPSII mutants 48 hours after a shift from non-EC (no bias applied) to EC (bias applied) condition. In the presence of bias, cells from biofilms (b) and planktonic cells (c) were separately analyzed. Pathway enzymes are sorted into categories based on their functions. From top to bottom, proteins are illustrated in more detailed categorization. Every tile (small polygon) represents one type of protein. Tile sizes represent the mass fractions of proteins. Shown are representative results from biological triplicates. All electricity and illumination supply were programed as “30 s supply + 30 min interval”.

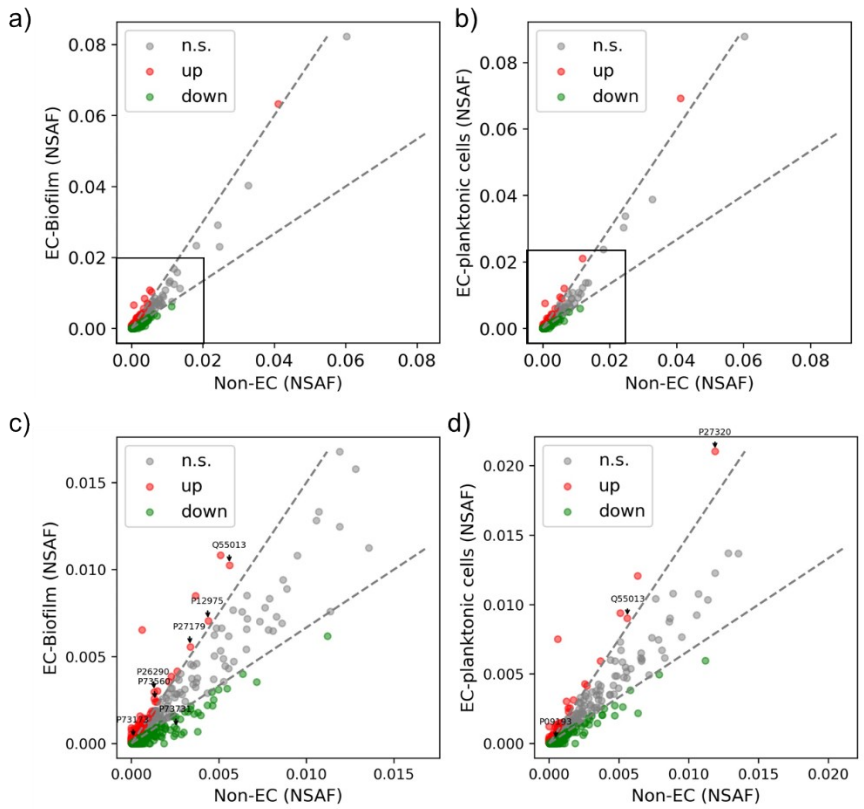

#Locus	Fold Change	Protein Name
P26290	2.28	Cytochrome b6-f complex iron-sulfur subunit 2
Q55013	1.83	Cytochrome c-550
P73560	1.78	Glycine cleavage system H protein
P73173	1.76	PilJ protein
P27179	1.66	ATP synthase subunit alpha
P12975	1.61	Photosystem I reaction center subunit IV
P73731	-3.08	Photosystem II reaction center Psb28 protein
P27320	1.79	Ferredoxin-1
P09193	-2.66	Photosystem II CP43 reaction center protein

Fig. S6. Scatter plot of relative protein levels for ΔPSII cells 48 hours after a shift from non-EC (no electricity applied) to EC (electricity applied) condition. The circles indicate the relative protein levels represented by the normalized spectral abundance factor (NSAF). Cells on the biofilm (**a** and **c**) and planktonic cells (**b** and **d**) were analyzed separately. The dashed lines indicate 1.5-fold increase or decrease in protein abundance. >1.5-fold changes are plotted in red (up) and green (down). The inner frames inside the **a** and **b** are amplified and shown as **c** and **d**, respectively. Arrows indicate the proteins that are potentially relevant to exogenous electron transfer or new CO_2-fixing pathway. Shown are representative results from biological triplicates. All electricity and illumination supply were programed as “30 s supply + 30 min interval”.

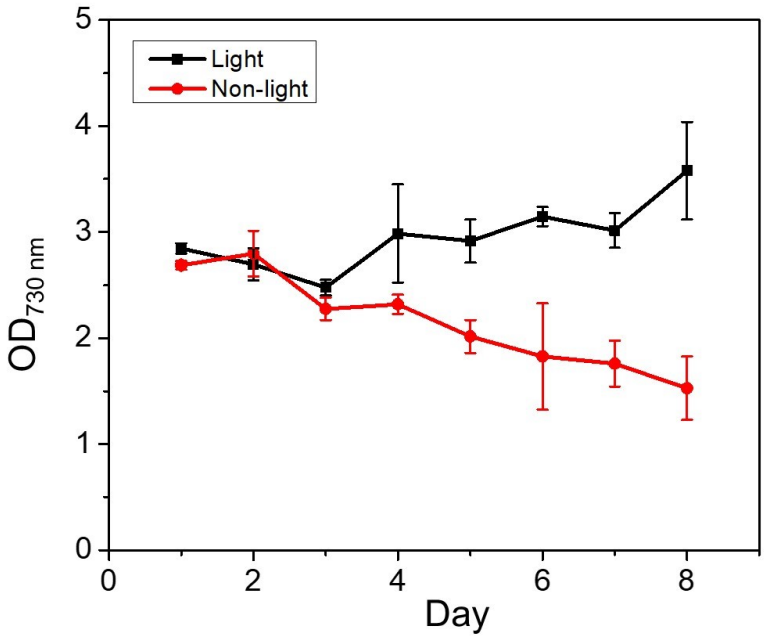

Fig. S7. OD_{730} of ΔPSII under external electrical bias 30s -0.7 V vs. Ag/AgCl EC with 30 min non-EC interval) with coordinated “30 s supply + 30 min interval” illumination and without illumination. Error bars represent standard deviations from biological triplicates.

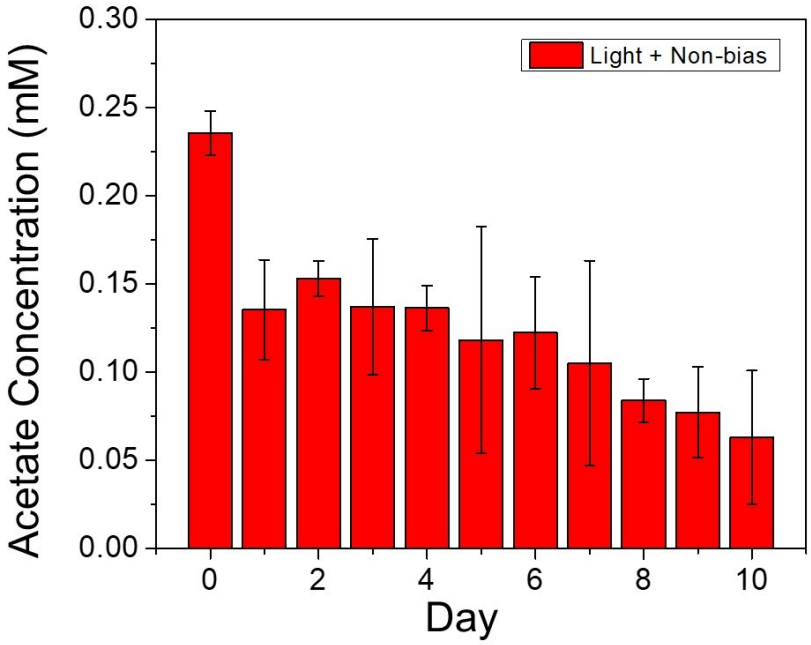

Fig. S8. Acetate concentrations in the light-illuminated (30 s supply + 30 min interval) culture of PSII deficient *Synechocystis* without external electrical bias. Error bars represent standard deviations from biological triplicates.

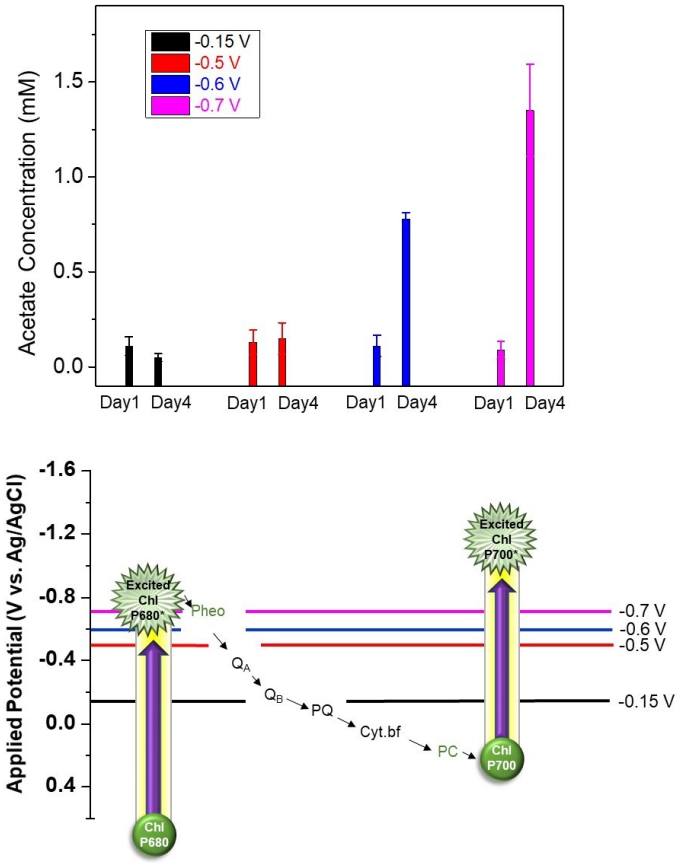

Fig. S9. Acetate production in PSII deficient *Synechocystis* (Top) as a function of applied potentials (-0.15 to -0.7V) based on their levels in the "Z" scheme of natural photosynthesis (Bottom). The electricity and illumination supply under all different potentials were programed as "30 s supply + 30 min interval". Error bars represent standard deviations from biological triplicates.

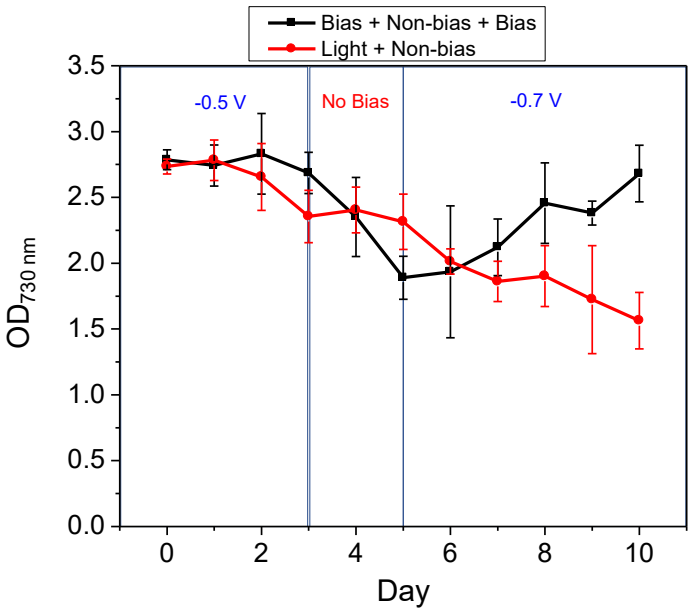

Fig. S10. OD_{730} of ΔPSII when external electrical bias was manipulated. The black curve shows the -0.5 V (vs. Ag/AgCl) bias applied for the first 3 days, no bias for next 2 days and then -0.7 V (vs. Ag/AgCl) bias applied for final 5 days under the illumination (white LED, 55 μmol m^{-2} s^{-1} on FTO glass). Red curve indicates the OD_{730} without external electrical bias under constant illumination. All electricity and illumination supply were programed as "30 s supply + 30 min interval". Error bars represent standard deviations from biological triplicates.

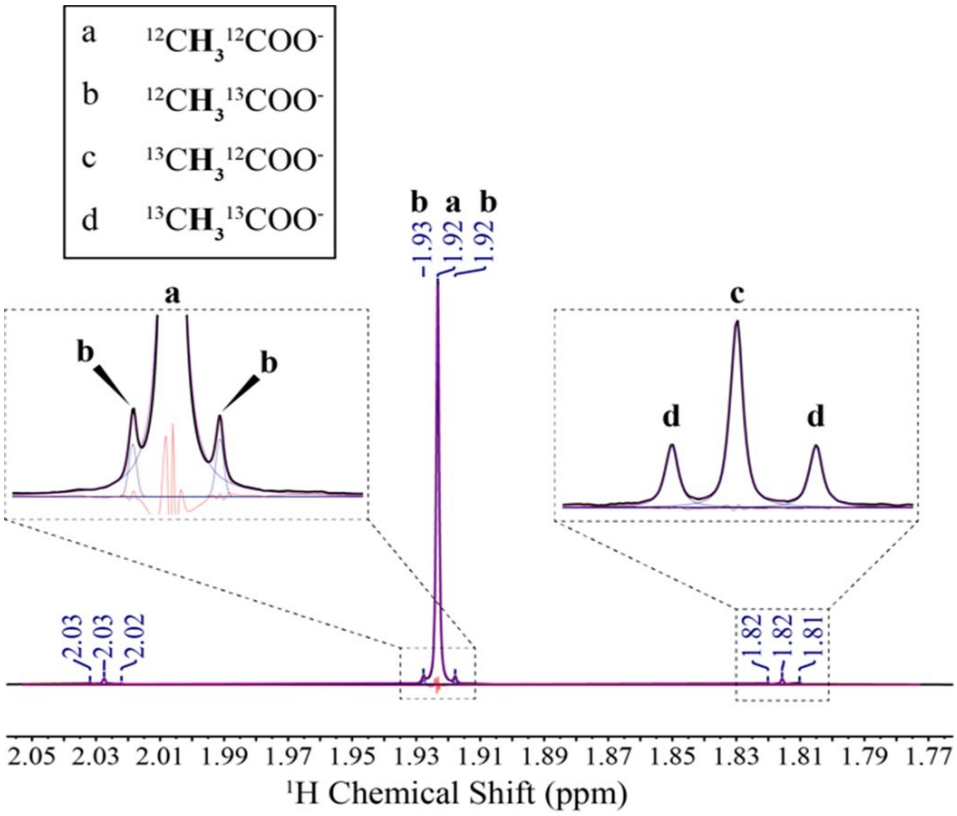

Fig. S11. ^{1}H-NMR spectra indicating the acetate was labeled in both methyl and carboxyl carbons from ^{13}C-bicarbonate. Samples are supernatant collected from the electrophototrophic system under illumination (white LED, 55 μmol m^{-2} s^{-1} on FTO glass) and intermittent external electrical bias supply (-0.7 V vs. Ag/AgCl) for 5 days. All electricity and illumination supply were programed as “30 s supply + 30 min interval”.

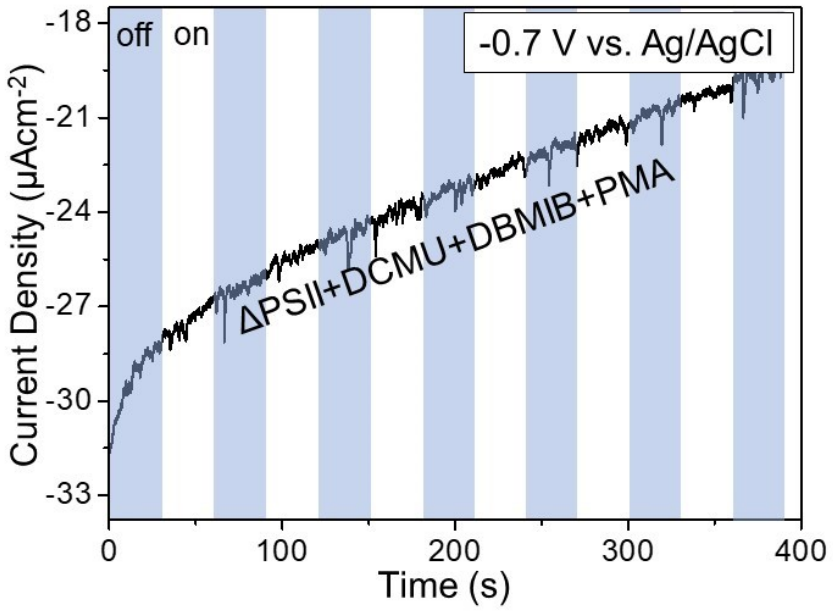

Fig. S12. The current response of culture with PSII mutant cells by adding all inhibitors (PMA, DCMU, and DBMIB) under the same chopped illumination condition as used in Fig. 2b. The electrochemistry experiments were conducted for 5 replicates and the results were reproduceable. A representative result is shown here.

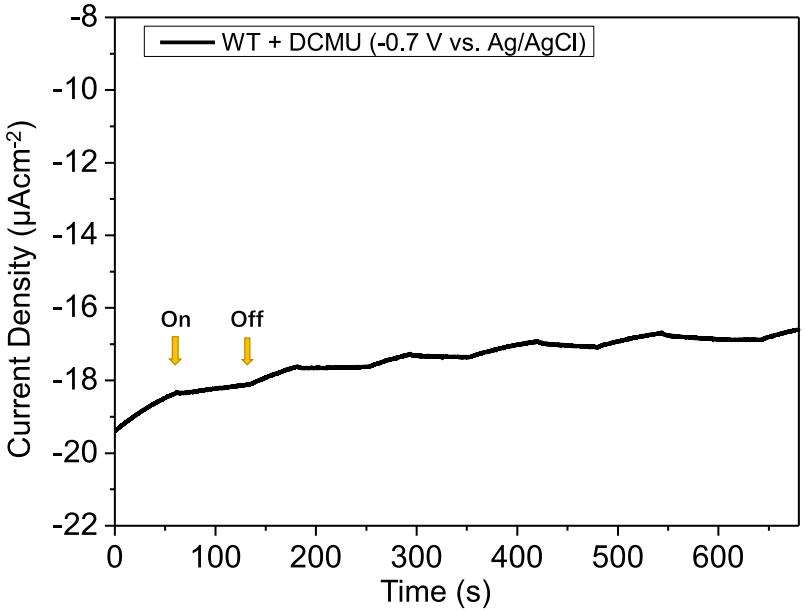

Fig. S13. The current response of a culture with wild-type (WT) cells and DCMU inhibitor under the same chopped illumination condition as the result shown in Fig. 2a. In order to ensure a reliable comparison, the electrolyte components are the same as those used for the culture in Fig. 2a. The electrochemistry experiments were conducted 5 times and the representative result is shown here.

Supplementary Text

Section S(I): Efficiency approximation

The inoculum was pre-incubated in the heterotrophic medium as discussed in the previous section. The energy consumed in the electrophototrophic reaction includes the external electrons taken by PSII deficient cyanobacteria and photoemission at PSI (Fig. S14). In order to quantify the conversion of electrons taken up by the PSII deficient cyanobacteria for CO_2 reduction, selective acetic acid generation from external electricity was defined as exocellular electrons uptake efficiency ($EEUE_{Acetate}$). The $NaH^{13}CO_3$ experiment data were used for this purpose. The CO_2 reduction to acetate follows the equation:

$$2CO_2 + 2H_2O \rightarrow CH_3COOH + 2O_2 \quad (1)$$

Producing one mole acetate need 8 electrons transfer. The $EEUE_{Acetate}$ value under electrophototrophic condition can be calculated based on the following equation:

$$EEUE_{Acetate} = \frac{8 \times \Delta n_{^{13}C\,-\,labeled\ Acetate} \times F}{\int Idt} \quad (2)$$

where $\Delta n_{^{13}C\,-\,labeled\ Acetate}$ is the number of moles of ^{13}C-labeled acetate produced over a given time *t*, *F* is the Faradaic constant, and $\int Idt$ is the amount of charge that has been passed through the working electrode during the sampling period by electrochemical potentiostat, which was 0.358 C. With the acetate concentrations of ~0.163 mM (initial) and ~0.817 mM (the 5th day) and corresponding ^{13}C-labeled acetate fractions of 0.1% (initial) and 5.25% (the 5th day) (Fig. 3c), the acetate concentration change in ~ 5 days is about 0.817 x 5.25% - 0.163 x 0.1% = 0.043 mM. The volume of the culture is 7 ml. As the result, the $\Delta n_{^{13}C\,-\,labeled\ Acetate} = 0.043\ mM \times 7\ ml = 2.99 \times 10^{-7}$ mole. Using the measured value of Coulombs accumulated this five-day electrophototrophic period (Fig. S15), the calculated average $EEUE_{Acetate}$ through electrophototrophic metabolism is 64.56 %.

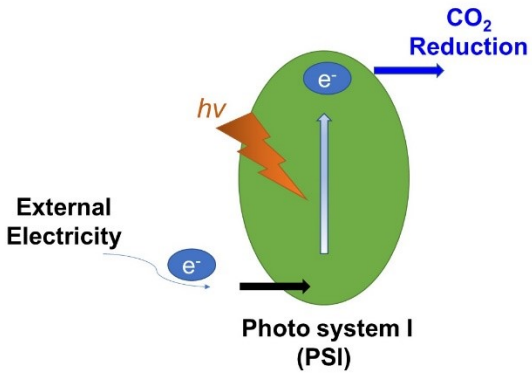

Fig. S14. Key electron transfer processes in electrophototrophic reaction.

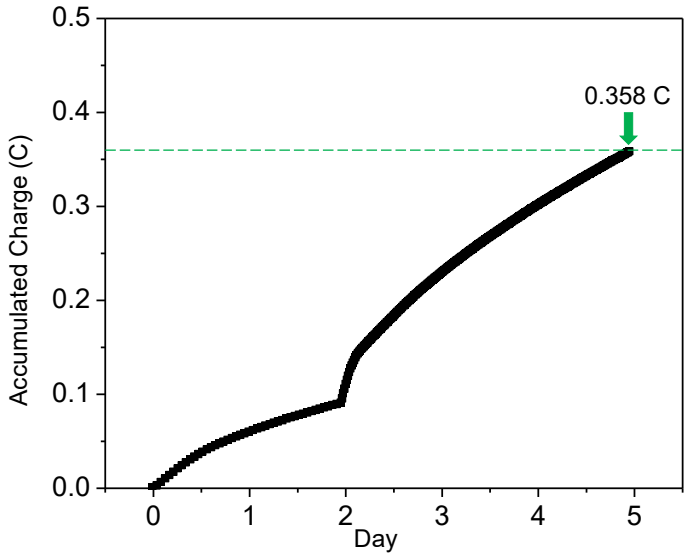

Fig. S15. Accumulated electrons transferred to hybrid electrophototrophic system within 5 days. Green arrow and dash line indicate the total charge consumed which is used in the energy efficiency calculation. All electricity and illumination supply were programed as “30 s supply + 30 min interval”.

In the ethylene producing experiment, the exocellular electrons uptake efficiency (*EEUE*$_{Ethylene}$) can be calculated by the similar method above. The CO_2 reduction to ethylene follows the equation:

$$2CO_2 + 2H_2O \rightarrow C_2H_4 + 3O_2 \quad (3)$$

Producing one mole ethylene need 12 electrons transfer. The *EEUE*$_{Ethylene}$ value under electrophototrophic condition can be calculated based on the following equation:

$$EEUE_{Ethylene} = \frac{12 \times \Delta n_{Ethylene} \times F}{\int Idt} \quad (4)$$

where $\Delta n_{Ethylene}$is the number of moles of ethylene produced over a given time *t*, *F* is the Faradaic constant, and $\int Idt$ is the amount of charge that has been passed through the working electrode during the sampling period by electrochemical potentiostat. The charge

transfer in the whole process was 3.655 C. With the ethylene amount of ~0 mole (initial) and ~2.36 x 10^{-6} mole (the 8th day), the ethylene change $\Delta n_{Ethylene} = 2.36 \times 10^{-6}$ mole. The calculated average $EEUE_{Ethylene}$ through electrophototrophic metabolism is 74.89 %.

Considering the illumination involved in this electrophototrophic process, the energy conversion efficiency approximation is conducted in similar fashion to approaches reported in previous literature[1]. Here we define the import energy to acetate efficiency as follows:

$$\eta = \frac{\left(\Delta_r G^0\right)\left(\Delta n_{^{13}C\,-\,labeled\ Acetate}\right)}{E_{electricity} + E_{illumination}} \tag{5}$$

where $E_{electricity}$ and $E_{illumination}$ are the energies provided by exogenous electricity and illumination, respectively, over time *t*. The Gibbs free energy of reaction ($\Delta_r G^o$) for CO_2 reduction to acetate can be calculated according to the following chemical reaction:

$2CO_2$ (g) + $2H_2O$ (l) → CH_3COOH (l) + $2O_2$ (g)

$$\Delta_r G^0 = \sum \Delta_f G^0 products - \sum \Delta_f G^0 reactants = 1015.32\ kJmol^{-1} \tag{6}$$

The applied electrochemical potential in the energy efficiency calculation is defined as the voltage difference between working and counter/reference electrodes in the two-electrode configuration for full-cell reaction.[1] In the three-electrode setup, the voltage of the full electrochemical reaction is defined between working and counter electrode, which was measured as ΔE^o = 3.2 *V*. If a two-electrode setup was applied for our experiment system, ~3.2 V induced a similar cathodic current passing the working electrode. Therefore, this potential can be used for the calculation of electricity energy applied on the bacteria cells. This electricity energy ($E_{electricity}$) that was supplied by an external source (potentiostat) passed over the course of our five-day experiment was equal to $\int Idt \times \Delta E^o$ = 0.358 C × 3.2 V = 1.144 J where 0.358 C is the total number of Coulombs passed over the experimental duration (7020 s, see the following discussion) (Fig. S15),

producing 2.99 x 10^{-7} mole acetate. 1 mole acetate requires the electricity energy: (1.144 J x 2.78 x 10^{-7} kWh J^{-1})/(2.99 x 10^{-7} mole) = 1.06 kWh $mole^{-1}$.

The illumination used in the experiment is the typical white LED illumination for algae growth (photobioreactor FMT150, photon systems instrument, Czech Republic). Photon flux was measured by Li-250A Light Meter with a quantum sensor (LI-COR Biosciences, NE, USA). The photon flux of the illumination was adjusted to 55 μmol $s^{-1}m^{-2}$ (3.3 x 10^{19} $s^{-1}m^{-2}$) (Fig.S16a) during the intermittent illumination (see the following discussion). After passing through the FTO and the carbon felt cathode and reaching the bacterial culture, the photon flux density decreased and was measured as ~12 μmol $s^{-1}m^{-2}$ (400 nm-700 nm).

The illumination energy ($E_{illumination}$) would be calculated with this photon flux by the following equations:

$$\Phi_\lambda = \frac{P_d^\lambda}{N_A E_{photon}^{\lambda}} \tag{7}$$

$$\Phi = \int \Phi_\lambda d\lambda \tag{8}$$

$$P_d = \int P_d^\lambda d\lambda \tag{9}$$

$$E_{illumination} = P_d t A \tag{10}$$

In these equations, Φ_λ is the photon flux at a certain wavelength, Φ is the photon flux integrated over the range of incident photon wavelengths, P_d^λ is the corresponding power density (W m^{-2}) at a certain wavelength, P_d is the integrated over the range of incident photon wavelengths, N_A is the Avogadro constant, E_{photon}^{λ} is the photon energy at a certain wavelength. t is the illumination time and A is the illumination area. As described above, the photon flux measured over the 400 nm-700 nm output of the LED source on the bacteria cells was Φ =12 μmol $s^{-1}m^{-2}$ (7.23 x 10^{18} $s^{-1}m^{-2}$). If the energy lost through the

carbon felt electrode was considered, the Φ = 55 μmol $s^{-1}m^{-2}$ (3.3 x 10^{19} $s^{-1}m^{-2}$) would be used to calculate the illumination energy applied on this electrophototroph device.

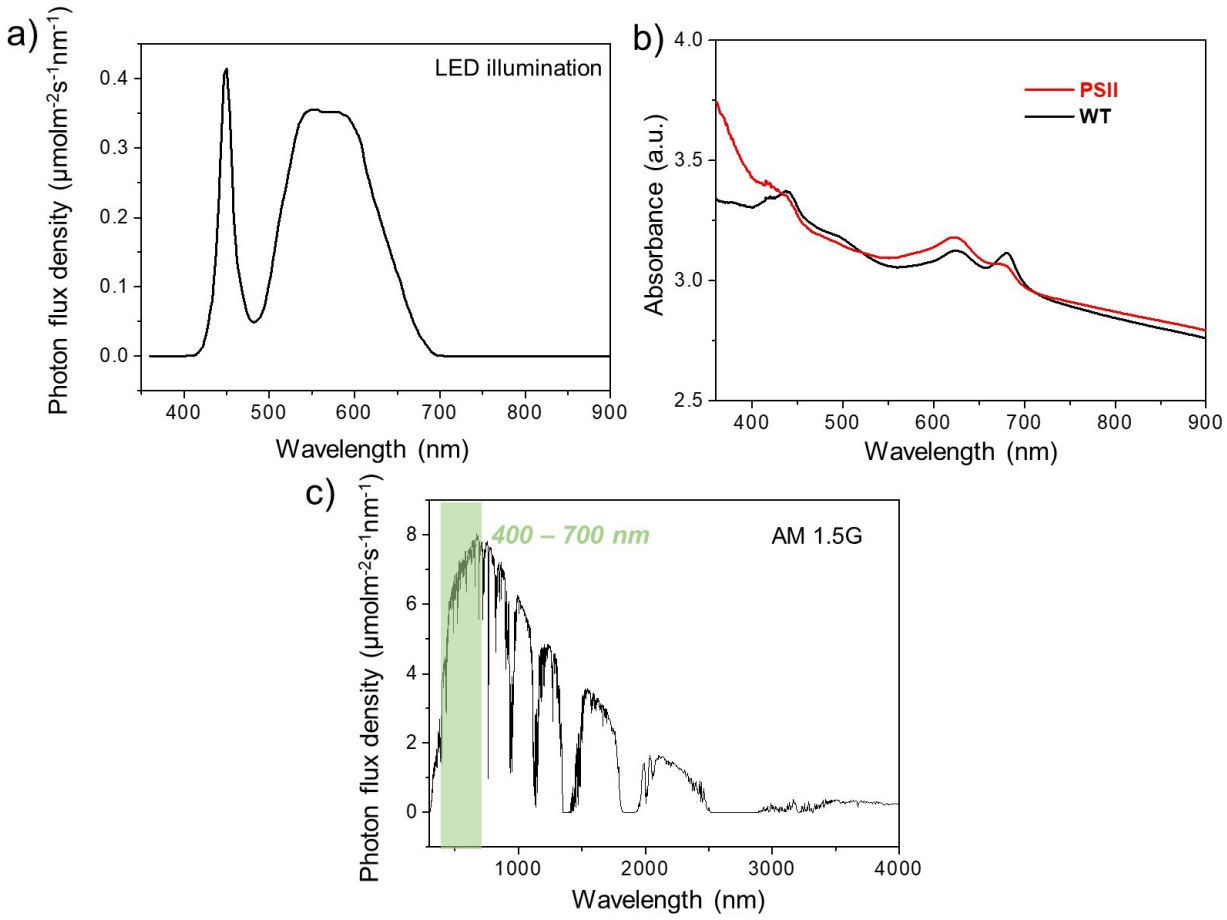

Fig. S16. a) The photon flux density spectrum with the measured value of ~55 μmol $s^{-1}m^{-2}$ ranging from 400 nm to 700 nm. b) the absorbance spectrum of the WT and PSII-mutant culture when the OD_{730nm} = 3. c) conventional AM 1.5G solar spectrum.

Based on the intermittent illumination and electron supply ("30 s illumination and electricity supply + 30 min interval"), the actually accumulated illumination time t = 30s × 234 cycles = 7020 s for ~ 5 days and FTO glass window area (1.152 cm^2) were determined. Therefore, the illumination energy ($E_{illumination}$) when the photon flux of 12 μmol $s^{-1}m^{-2}$ irradiated on the bacteria cells was 2.13 J. The total import energy to acetate efficiency η = ~ 9.29 % while the photon energy to acetate efficiency is 14.29 %. This illumination energy received by the whole electrophototroph device is even larger (~9.68

J) because the higher illumination photon flux (55 μmol $s^{-1}m^{-2}$). In this case, the total import energy and photon energy to acetate efficiencies reduced to 2.81 % and 3.14%. Table S1 summarizes the efficiency results based on three bio-replicates under different efficiency definitions.

Based on reported methods[1], since the reaction proceeds at 30 °C, the Gibbs free energy compared to the above standard condition should also incorporate the relevant entropy changes, which are assumed to only arise from entropy changes of gaseous CO_2 and O_2 in our reaction.

$$\Delta S_{rxn}^{\ 0} = -\left(\frac{\partial G}{\partial T}\right)_{P,\,C} = \Delta S^0 products - \Delta S^0 reactants$$

$$= 2\Delta S^0(O_2) - 2\Delta S^0(CO_2) = -17.2\ J\ mol^{-1}K^{-1} \quad (11)$$

So, the Gibbs free energy change (ΔG) with temperature change from room temperature to incubation temperature is $-\Delta S_r^0 \Delta T/\Delta_r G^0$=0.0152 % increase, resulting the neglectable increase of η.

Table S1. Summary of approximately calculated energy conversion efficiencies to acetate on cyanobacterial cells and electrophototrophic device.

Efficiency \ Object	Over Cyanobacteria Cells	Over Electrophototrophic Device
Exocellular electrons up-taken efficiency ($EEUE_{Acetate}$)	64.56 ± 4.15 %	64.56 ± 4.15 %
Import energy to acetate efficiency (η)	9.32 ± 0.37 %	2.82 ± 0.16 %
Photon energy to acetate efficiency	14.38 ± 0.88 %	3.16 ± 0.19 %

Section S(II): Intermittent electrons supply for electrochemical incubation

To realize exogenous electron-driven CO_2 fixation and conversion, we incubated PSII-deficient cyanobacterial cultures and applied electrical potential with amperometric

characterization. Light and electrical bias were investigated. In practice, we found that the increase of accumulated charges supplied to bacterial cells would become slower over time when continuously providing electricity in electrophototrophic process (Fig. S17). The acetate production did not sustain during this process. Ceasing the electricity supply while maintaining the illumination for a certain period could effectively resume the electrophototrophic process. This observation indicates a mismatch occurring between fast injection of exogenous electrons and slow charge transfer in PETC. We speculate that persistent supply of exogenous electrons might over-reduce the redox components in PETC, the re-oxidation of which largely relies on electron consumption in downstream metabolic activities. However, if reoxidation proceeds more slowly than the rate of external electron input, this imbalance may leave the PETC redox carriers in a more reduced state, retarding continuous influx of exogenous electrons over time. Illumination of the biotic system would allow electrons to be consumed during metabolism, therefore regenerating oxidized PETC components that could readily accept additional exogenous electrons. On the other hand, continuous illumination with insufficient exogenous electron supply could also result in an unmatched electrophototrophic process (see Fig. S18). These observations suggest that a good coupling of exogenous electron injection kinetics with the biological photosynthetic metabolism will be crucial for the electrophototrophic process.

Based on this analysis, we developed “intermittent electrons supply” as a strategy. As shown in Fig. S17, much higher charge transfer rate and acetate productivity can be achieved when 30 minutes interval was introduced between 30 second electricity supply than the continuous supply condition. We thus adopted the “30 s + 30 min” electricity supply in the electrochemical chamber for long-term electrophototrophic incubation. The illumination was programmatically controlled as intermittent irradiation (“30 s illumination + 30 min interval”), coordinating with the electricity supply. In Fig. S17, all illumination conditions were constant as “30 s illumination + 30 min interval” while the electricity supplies varied. In Fig. S18, all bias conditions were constant as “30 s supply + 30 min interval” while the illumination supplies varied.

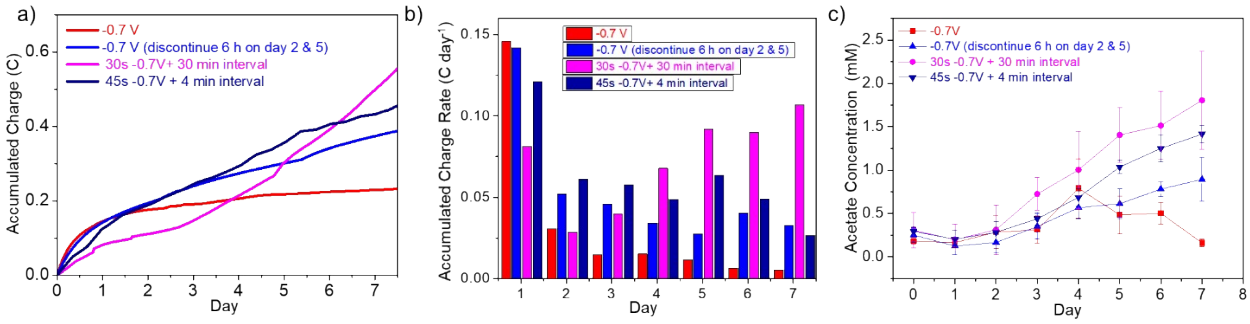

Fig. S17. Effect of energetic supplies to the electrophototrophic hybrid-1. Input is intermittent illumination (white LED, 55 μmol m^{-2} s^{-1}, 30 s illumination + 30 min interval) with 4 programmed electricity supplies. **a)** Time courses of accumulated charge transfer to ΔPSII. **b)** Daily rates for charge accumulation. The rate for continuous electricity supply (red bar) gradually decreased over time, while intermittent electricity supply (e.g., 30s -0.7 V vs. Ag/AgCl EC with 30 min non-EC interval, pink bar) can maintain more stable charge transfer to the cyanobacterium over time. **c)** Time courses of acetate production.

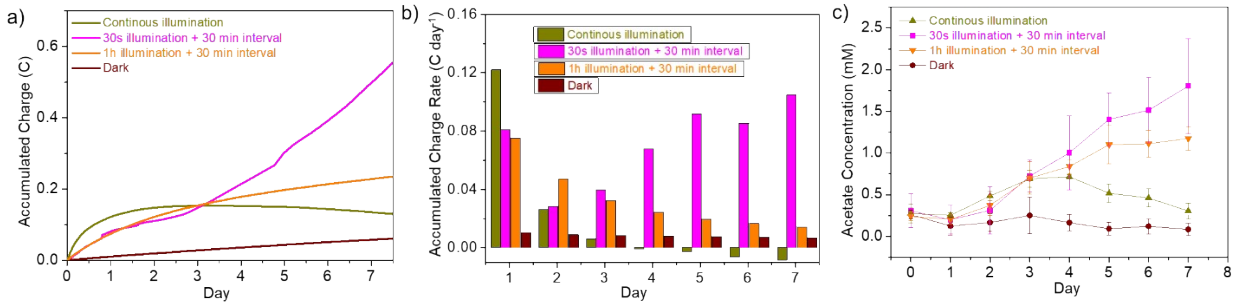

Fig. S18. Effect of energetic supplies to the electrophototrophic hybrid-2. The input here is constantly intermittent electricity (30s -0.7 V vs. Ag/AgCl EC with 30 min non-EC interval) with 4 altered light conditions. **a)** Time courses of accumulated charge transfer to ΔPSII in 3 different illumination conditions (white LED, 55 μmol m^{-2} s^{-1}) and in dark. **b)** Daily rates for charge accumulation. **c)** Corresponding time courses of acetate production with or without illumination.

Section S(III): Potential vision and associated challenges of electrophototroph-photovoltic hybrid concept

From a broad standpoint, this work validates the first step of a new photosynthesis concept to elevate the photosynthesis efficiency ceiling: Powering single a light-absorbing photosystem (PSI) *via* exogenous electricity which can be generated by PV with extended range of solar energy absorption. Increases in efficiencies might be obtained by PV devices that use the blue and near-UV region of the solar spectrum more effectively or capture the energy of the sub-bandgap IR photons (illustrated in Fig. S19)[2]. Solar energy that includes only UV and IR irradiation could provide exogenous electrical energy while 400-700nm solar photons could photoexcite cyanobacterial PSI to synergistically drive electrophototrophic CO_2 reduction. To turn this concept into reality, technical challenges still exist in the current electrophototrophic system. The requirement of pulsed illumination and electricity supply implies that the photon/electron transfer in the hybrid system could be suboptimal. While the solar panels function well with continuous illumination, the currently employed bacteria do not. The design of an appropriate switching scheme to divert some portion of the total electricity delivered by a solar panel to the cyanobacteria could be one possible solution to match the continuous solar illumination to pulsed supply of electrophototrophic system. Other potential challenges include the efficient delivery of solar illumination to liquidous cultures and the design of practical devices to coordinate hybrid photosynthesis under the required illumination conditions[3].

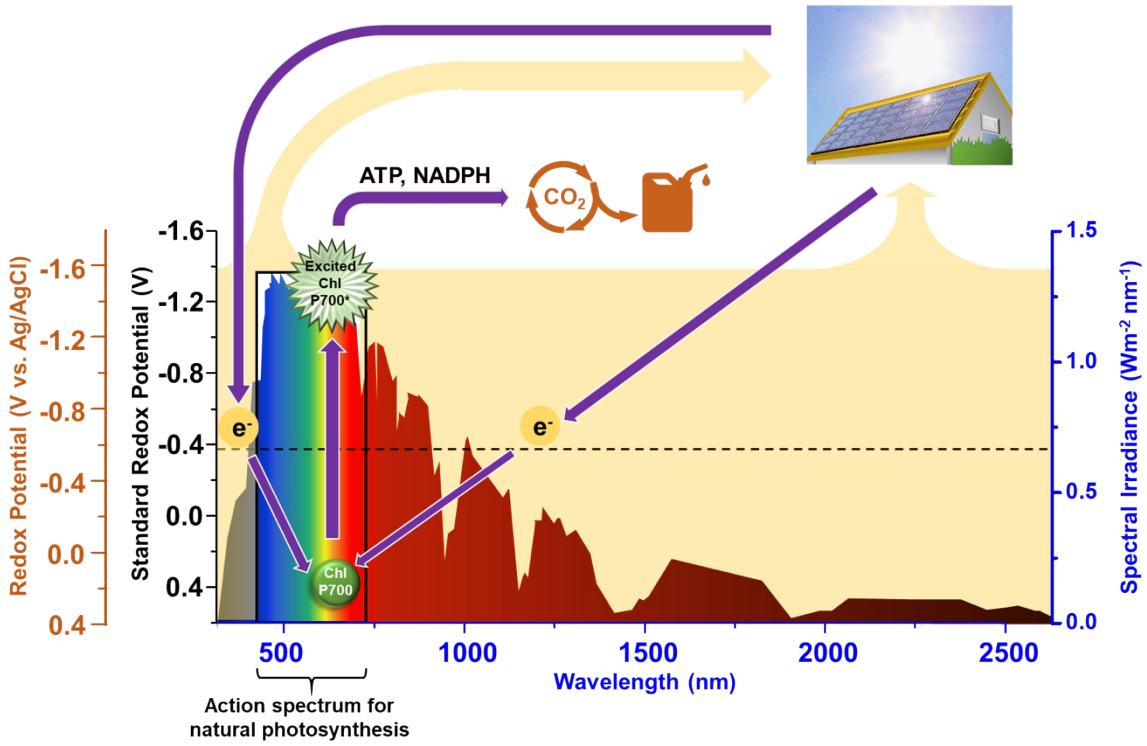

Fig. S19. Schematic illustration of a hybrid photosynthesis system to convert broader spectrum of PAR than natural photosynthesis. Leveraging PV device, UV-blue and IR regions that cannot be utilized by photosynthetic organisms, may be converted to electricity to energize electrophototrophic cyanobacteria with single PSI for CO_2 valorization. Dash line represents the standard redox potential where the exocellular electrons shuttled to the photosynthetic cells carrying a single photosystem.

Table S2. MDV of proteinogenic amino acids in PSII deficient *Synechocystis* under biased (-0.7 V vs. Ag/AgCl) and unbiased conditions.

MDV		m0	m+1	m+2	m+3	m+4	m+5
Ala_57(PYR1-3)	Biased	0.91261	0.07920	0.00692	0.00127	0	0
	Unbiased	0.96247	0.03618	0.00001	0.00134	0	0
Ala_85(PYR2-3)	Biased	0.96666	0.02754	0.00580	0	0	0
	Unbiased	0.98055	0.01944	0.00001	0	0	0
Ser_57(PGA1-3)	Biased	0.92125	0.06662	0.00946	0.00267	0	0
	Unbiased	0.95670	0.04327	0.00001	0.00001	0	0
Ser_85(PGA2-3)	Biased	0.94565	0.03507	0.01928	0	0	0
	Unbiased	0.97935	0.02064	0.00001	0	0	0
Gly_57(SER1-2)	Biased	0.29693	0.66770	0.03537	0	0	0
	Unbiased	0.97242	0.02758	0.00001	0	0	0
Gly_85(C1)	Biased	0.63306	0.36694	0	0	0	0
	Unbiased	0.99025	0.00975	0	0	0	0
Glu_57(2OG1-5)	Biased	0.79504	0.19492	0.00742	0.00148	0.00070	0.00045
	Unbiased	0.92860	0.07125	0.00001	0.00001	0.00001	0.00011
Asp_57(OAA1-4)	Biased	0.77960	0.16755	0.04555	0.00001	0.00729	0
	Unbiased	0.92537	0.07305	0.00001	0.00045	0.00112	0
Phe_302(PEP1-2)	Biased	0.92676	0.06637	0.00687	0	0	0
	Unbiased	0.96572	0.03427	0.00001	0	0	0
Thr_57(OAA1-4)	Biased	0.74364	0.22885	0.01414	0.000004	0.01336	0
	Unbiased	0.92519	0.06412	0.00597	0.00471	0.00001	0

Supplementary Material References

1. C. Liu, B. C. Colon, M. Ziesack, P. A. Silver and D. G. Nocera, *Science*, 2016, **352**, 1210-1213.
2. R. E. Blankenship, D. M. Tiede, J. Barber, G. W. Brudvig, G. Fleming, M. Ghirardi, M. R. Gunner, W. Junge, D. M. Kramer, A. Melis, T. A. Moore, C. C. Moser, D. G. Nocera, A. J. Nozik, D. R. Ort, W. W. Parson, R. C. Prince and R. T. Sayre, *Science*, 2011, **332**, 805-809.
3. D. Spasiano, R. Marotta, S. Malato, P. Fernandez-Ibañez and I. Di Somma, *Applied Catalysis B: Environmental*, 2015, **170-171**, 90-123.